Feedback Control for Counterflow Thrust Vectoring

Emmanuel G. Collins, Jr., Yanan Zhao, Farrukh Alvi, Mohammed I. Alidu and Paul J. Strykowski

Abstract— **Thrust vector control is used to increase the maneuverability of aircraft. In current aircraft it is implemented using movable control surfaces such as vanes and flaps. Counterflow thrust vectoring (CFTV) is a fluidic approach to thrust vectoring that has the potential to improve on the conventional approaches by reducing weight and increasing the reaction speed. Open loop implementation of CFTV has been demonstrated in laboratory settings. However, ultimately this technology must be implemented using feedback control. This paper describes an experiment for developing feedback control technology for CFTV. It is seen that the key compensation issues are parameter uncertainty, transportation delay, and hysteresis (for certain CFTV geometries). Initial results on system identification are described along with potential control design methodologies.**

I. INTRODUCTION

The maneuverability of aircraft is traditionally achieved by the use of aerodynamic control surfaces such as ailerons, rudders, elevators and canards. The deflection of these surfaces modifies the exterior shape of the vehicle in critical points of its structure, thus creating a change in the aerodynamic forces acting on the vehicle and causing it to maneuver [6].

Thrust vector control (TVC) is a more recent technology that increases vehicle maneuverability by directly changing the direction of the thrust force vector. This approach has been successfully implemented on several military aircraft and has resulted in increased roll rates and enhanced maneuverability at low speed, high angle of attack flight conditions where aerodynamic surfaces are very ineffective. TVC can also reduce the distance necessary for take off and landing or even make vertical take off and landing possible.

Current implementation of TVC employs movable control surfaces such as vanes and/or flaps arrayed around the nozzle exit to redirect the jet exhaust. The mechanical actuators and linkages used to change the thrust vector angle add weight and complexity to the aircraft, which leads to increased cost and maintenance requirements. In addition, the dynamic response of the jet is limited by the response of the mechanical actuators used and the thrust losses are not small [2], [4], [6]. A promising alternative approach is fluidic thrust vectoring, where a secondary air stream is employed to redirect the primary jet. Fluidic thrust vectoring requires few or no moving parts in the primary nozzle; therefore it simplifies the hardware, reduces weight and maintenance needs. In addition, it has the fast dynamic response inherent to fluidic devices [1], [4], [6].

Counterflow thrust vectoring (CFTV) was first proposed in [3]. It is a technique that is different than other fluidic techniques so far proposed. Instead of having a secondary air stream flowing into the nozzle, CFTV uses a secondary flow traveling in the opposite direction to that of the primary jet. Recent engineering research has successfully demonstrated the potential of thrust vector control using counterflow at conditions up to Mach 2 [1], [2], [5]. However, since fluidic concepts in general are bistable and hysteretic in nature, CFTV has some limitations. In particular, for certain CFTV geometries the primary jet tends to attach itself hysteretically to the suction collar at certain conditions. When this occurs, control of the thrust vectoring angle is lost. This *attachment* is difficult to overcome without large changes in flow conditions [4]. A jet with a design Mach number 2 was used in this research because considerable experimental results are available to the authors at this Mach number. However, it should be noted that counterflow thrust vectoring has also been demonstrated at other Mach numbers, for example, Mach number 1.4 [6].

Past studies of CFTV have focused exclusively on the open loop behavior. However, for practical implementation it is vital that the counterflow scheme be used in conjunction with feedback. Hence, the primary objective of the research reported here is to design and implement effective feedback control laws for CFTV. Figure 1 illustrates that the CFTV feedback control loop constitutes an important minor loop of the overall aircraft attitude control. The control system must achieve fast slew rates by compensating for the transportation delay in the presence of significant parametric uncertainty. In addition, for certain CFTV geometries it must be able to compensate for the hysteresis that occurs when the counterflow is effectively stopped at attachment.

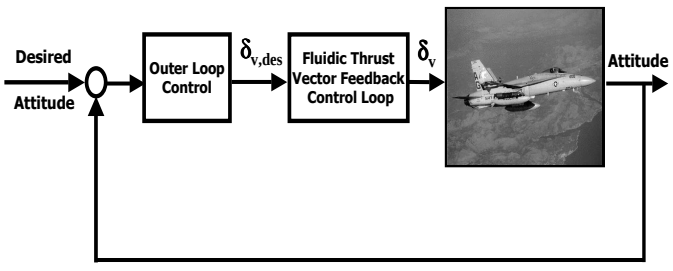

Fig. 1. Aircraft attitude control using fluidic thrust vector control

The authors have successfully constructed a testbed for investigating feedback control of CFTV. The characteristics of the current experiment have been shown to match those

This research was supported in part by the Air Force Office of Scientific Research under Grant F49620-01-0550.

The first four authors are with Department of Mechanical Engineering, Florida A&M University - Florida State University, Tallahassee, FL 32310 ecollins, yzhao, alvi, inenhe@eng.fsu.edu

The fifth author is with Department of Mechanical Engineering, University of Minnesota, Minneapolis, MN 55455 pstry@me.umn.edu

in the literature [1], [6]. Preliminary system modeling and analysis has been conducted and control law design for the system has commenced.

The paper is organized as follows. Section 2 describes some of the details of the CFTV concept along with the experimental testbed that is being used for feedback control development. Section 3 presents preliminary system modeling and analysis results. Section 4 discusses different candidate control approaches. Finally, Section 5 presents some conclusions.

II. DESCRIPTION OF COUNTERFLOW THRUST VECTORING (CFTV) AND THE EXPERIMENTAL TESTBED

This section first describes the concept of CFTV. It then describes an experimental testbed for investigating feedback control of CFTV.

A. Counterflow Thrust Vectoring

The basic geometry of a CFTV device, used for pitch vectoring, is illustrated in Figure 2. The collars are placed on either side of the primary flow nozzle (top and bottom in the figure) creating gaps between the exhaust jet and the collar surfaces which are curved away from the jet axis in the streamwise direction. To achieve upward thrust vectoring at an angle δ_v, a secondary counterflow must be established between the primary jet and the collar surface, creating a continuous flow path between the surrounding ambient fluid and the vacuum system. The action of counterflow in the upper shear layer gives rise to asymmetric entrainment and a cross-stream pressure gradient sufficient to vector the jet [1]. When the vacuum system is activated, creating counterflow in the gap between jet and the collar, continuous thrust vectoring can be achieved [1]. Previous experimental studies have demonstrated continuous control for values of δ_v up to 16 degrees [6]. In this figure, G represents the gap height and H is the nozzle height.

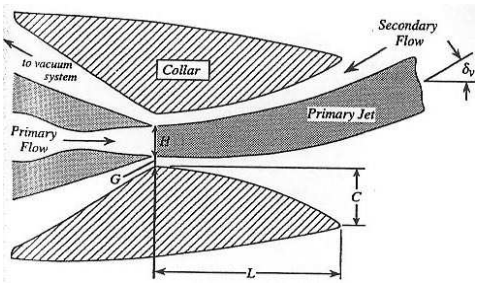

Fig. 2. Schematic of counter-flow thrust vector control

It is important to recognize that the thrust vectoring angle cannot be directly measured in practical implementation of CFTV, although experimental techniques do allow its measurement in laboratory settings. However, it has been shown that the pressure parameter $\frac{\Delta P_G A_{side}}{\rho_1 {U_1}^2 A_{jet}}$, which is essentially a non-dimensional ratio of the side force acting on the collar and the axial force imposed by the jet, has a nearly linear relationship to the thrust vector angle over a wide range of conditions [1] as shown in the thrust vector response curve in Figure 3. Here P_G is the pressure established in the secondary stream as measured in the jet exit plane on the collar surface, ΔP_G is the static negative gauge pressure in the jet exit plane on the collar surface (i.e., $\Delta P_G = P_{atm} - P_G$, where P_{atm} represents the absolute atmospheric pressure), A_{side} is the collar side area, ρ_1 is the primary jet density, U_1 is the primary jet velocity, and A_{jet} is the jet area at the nozzle exit. Thus, in practice ΔP_G will be selected as the command variable.

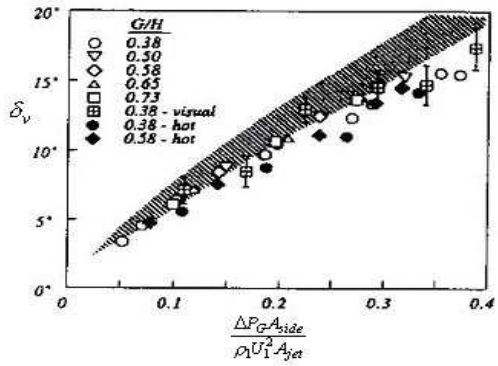

Fig. 3. Thrust vector performance

For certain CFTV geometries, if the pressure on the collar wall drops too much (i.e., ΔP_G becomes very large), the deflection of the jet will be too severe and it will attach to the wall. If this happens, continuous control of the jet is compromised since at this time thrust vectoring angle would generally jump to a value near the collar terminal angle. Jet attachment is a hysteretic phenomenon as once the jet is attached to the collar, change in the secondary flow has little effect on the thrust vectoring angle, and simply reducing the counterflow rate to reduce ΔP_G back to the value at which jet attachment occurred is not sufficient to release the jet from the collar [4]. It is generally necessary to entrain open air to the system to release the jet from the collar. Figure 4 shows a sketch of the hysteresis describing δ_v vs ΔP_G.

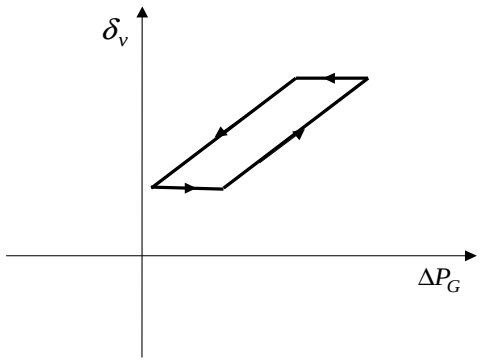

Fig. 4. Sketch of hysteresis

B. Experimental Testbed

The authors have constructed an experimental testbed to conduct feedback control research for CFTV as shown in Figure 5. It has five major parts: a jet, a collar, a control valve, two pumps and the pipe connections.

The rectangular Mach 2 jet in the exit plane has a width of 32.5 mm and a height of 5 mm. The inner contour of the collar is an arc of constant radius of curvature swept through an angle α and extending downstream of the nozzle exit for a distance given by $L = R\sin\alpha$, where $L = 34$ mm, $R = 78.5$ mm and $\alpha = 25.6$ deg.

The forward stream to the jet is supplied by a high-displacement reciprocating compressor, which is capable of supplying air at a maximum storage pressure of 160 bars. The vacuum source for the counterflow is provided by two Fuji VFC804A-7W pumps mounted downstream of the test rig.

To implement the feedback control, a control valve is installed between the collar and pumps to control the counterflow, which determines the thrust vector angle. A model 27N pneumatic R-DDV servovalve from HR Textron is used in the test rig for this purpose.

Data acquisition and control are implemented using dSPACE, which consists of a DS2002 A/D board, a DS2102 D/A board, a DS1005 PPC board, and a PX10 expansion box. To monitor the jet pressure (which should be 115 psi for a Mach 2 jet), a Validyne multiple range pressure transducer (model DP15TL) is used. There are 11 static pressure taps along the collar wall, and the multiple pressure measurements required to determine the collar static pressure distribution is facilitated by a Scanivalve model OED2 pressure sampling scanner.

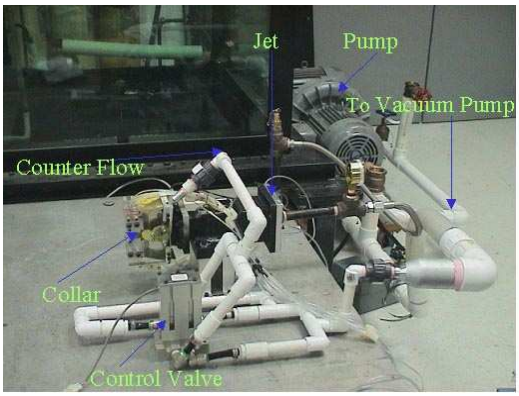

Fig. 5. Experimental testbed for feedback control

A schematic functional diagram of the testbed is shown in Figure 6. Please note that the two pumps can be connected in series as shown in the figure, or they can be used separately, i.e., either of the pumps can be disconnected from the testbed.

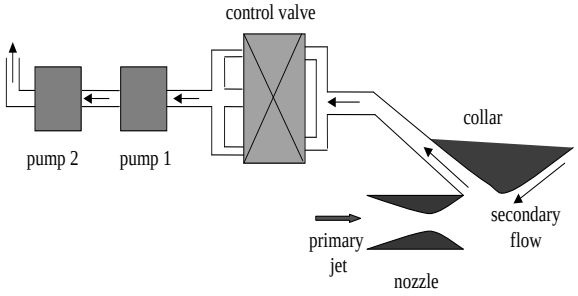

Fig. 6. Schematic functional diagram of the testbed

III. SYSTEM MODELING AND ANALYSIS

The first step in designing high performance control laws is to develop a model of the system. Since the detailed physics of CFTV are not entirely understood, it is necessary to obtain a model of the CFTV process using system identification based on input-output data.

A. Process Estimation

The model required for feedback control design has the voltage to the control valve as the input and the command variable ΔP_G as the output. An open-loop step response curve was obtained for a 5 volts step input applied at $t = 10$ sec. The test was run with only the first vacuum pump being turned on and a ratio of $G/H = 0.38$. Figure 7 shows the original response of the system with the output as P_G. Figure 8 represents this response by plotting the output as ΔP_G with the time axis shifted so that $t \leftarrow t - 10$ sec. Notice that Figures 7 and 8 reveal that the sensor used to measure the gap pressure P_G is very noisy. This makes the system identification process more difficult. Steps have been taken to minimize the sensor noise for future experiments.

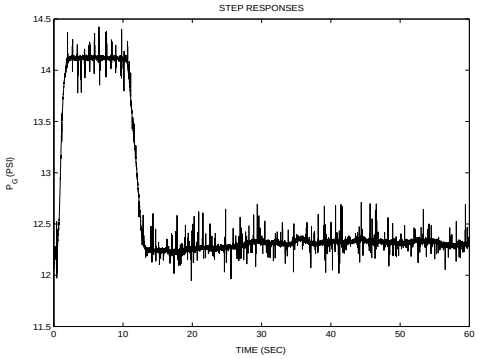

Fig. 7. Original step response of the system

A first order lag plus delay (FOLPD) model was first used to fit the response curve. Four experimental off-line estimation methods were used to estimate the FOLPD model, $\frac{K_p}{Ts+1}e^{-Ls}$, where K_p is the process static gain, T is the time constant and L is the time delay. The first method used was the graphical method proposed by Astrom and Hagglund [9], where K_p is chosen as the ratio of the steady state value of the step response over the amplitude

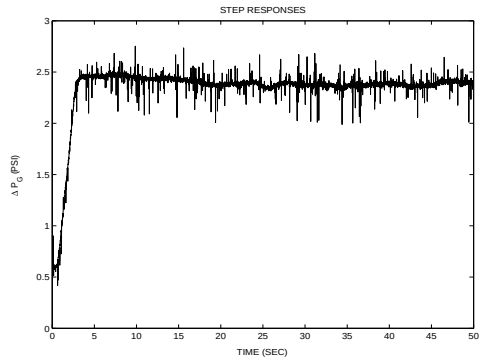

Fig. 8. Converted step response

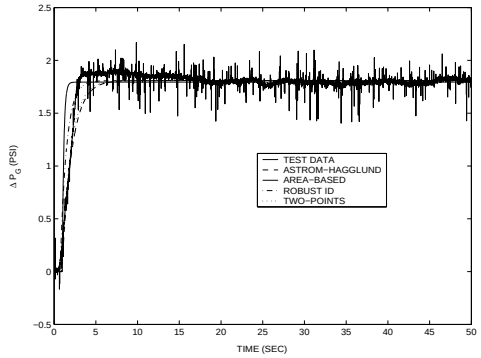

Fig. 9. Comparison of the estimated parameters with different approaches

of the step input, L is the intercept of the tangent to the step response curve that has the largest slope with respect to the horizontal axis, and T is the difference between the time when the step response reaches $0.63K_p$ and the time delay L. The second method used is the area-based method of [8], where process parameters are obtained by computation of characteristic areas. The third method used is a robust identification method that uses linear regression equations with instrumental variable least-squares method curve fitting [9]. The fourth method used is a two point method by Shaw [10], that obtains the time delay and time constant from the time taken to reach 28.4% and 63.2% of its steady state value.

TABLE I

PROCESS PARAMETER ESTIMATION

Estimation Methods	K_p	T	L
Astrom and Hagglund	0.3618	1.2	0.9333
Area-based	0.3588	0.1793	0.9829
Robust identification	0.3616	0.7580	0.7069
Two-point method	0.3618	1.1194	0.8806

Table I lists the process parameters obtained by the four approaches described above. The simulated step response obtained using the FOPLD models with the estimated process parameters were compared with the measured data as shown in Figure 9. It is seen that the area-based method resulted in a much faster time constant, revealing that this method is not robust with respect to the sensor noise appearing in the step response. Also, it is seen that the FOPLD models are not able to closely match the transient response of the system. Because of this, a second order model was developed to represent the system dynamics.

The second order system with time delay is of the form, $\frac{K_p}{T^2s^2+2T\xi s+1}e^{-Ls}$, where ξ is the damping ratio of the system. A method proposed in [11] was used to estimate the process parameters. The results yielded $K_p = 0.3618$, $T = 0.8539$, $\xi = 0.688$ and $L = 0.4583$. A comparison of the simulated data with the test data is shown in Figure 10. It is seen that a second order plus delay model closely matches the transient response of the system.

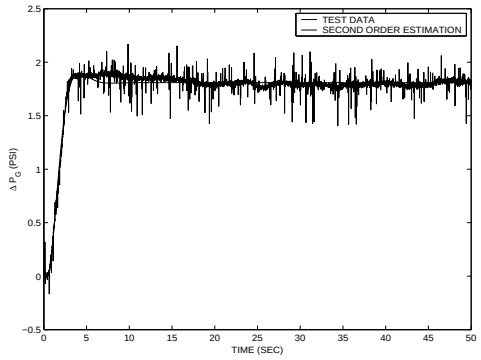

Fig. 10. Second order system estimation

B. Time Delay, Parameter Variations and Nonlinearity

The system time delay, parameter variations, and nonlinearities will have a major impact on the control design process for CFTV. The following provides a discussion of these observed features of the dynamic response of the CFTV.

1) Variability in the Steady State Gain: The CFTV testbed has been dynamically tested for step inputs of amplitudes 0 volt, 1 volt, $\cdots$, 5 volts. (The range of the control valve voltage is [0, 5] volt.) The resulting step responses are shown in Figure 11. Preliminary analysis has shown that each of the step responses of Figure 11 has approximately the same time constant and time delay. However, nonlinearity exists as evidenced by the nonuniform changes in the variability in the steady state output responses, detailed in Table II. The tests were run with only the second pump on (in replacement of the first pump) and $G/H = 0.38$. Due to the power limitation of the second pump, there is disaccord between the static gain under 5 volts and that of Section III.A.

It is currently conjectured that this variability in the steady state gain is a result of nonlinear losses in the control valve. Ongoing experiments are testing this hypothesis. The parameters of the dynamic model also vary with Mach number, jet pressure and jet temperature. For example, the jet pressure is supposed to be 115 psi for a Mach 2 jet engine. However, experimental observation shows

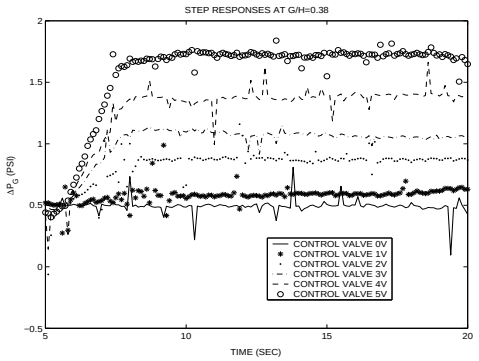

Fig. 11. Open-loop step responses under different control valve voltage

TABLE II
STEADY STATE GAIN AT DIFFERENT SETPOINTS

Amplitude of the Step Signal (volt.)	K_p
1	0.1050
2	0.1936
3	0.1922
4	0.2228
5	0.2460

that the jet pressure drops about 2 psi after 3 minutes of operation. It has also been observed that jet air temperature variation results in uncertainties in the collar pressure. For example, colder supplied air leads to lower collar pressure. Hence, additional parametric uncertainties are present in the CFTV system. This uncertainty is being quantitatively characterized in ongoing experiments.

2) Time Delay: The current system reveals a significant transportation delay as shown in Figures 7, 8, and 11. This delay is transportation delay related to the time it takes the counterflow to travel from the collar to the control valve. To achieve fast slew rates, this delay must be compensated.

3) Hysteresis: As discussed above, jet attachment is a hysteretic phenomenon, and whenever it occurs the continuous control of the thrusting angle becomes impossible. Jet attachment can be avoided by appropriate system design. In particular if the ratio G/H is sufficiently large, attachment may be avoided. However, it has been demonstrated that this type of geometry leads to smaller achievable thrust vector angles. Hence, if the larger thrust vector angles are required, then it is necessary to design control laws that are able to yield good performance in the presence of hysteretic attachment.

IV. CONTROL APPROACHES

Hyseteresis is a nonlinearity for which traditional control methods are insufficient [15]. However, CFTV can be continuously controlled under certain conditions. Hence, control law design will first be developed assuming hysteresis does not occur. The design objective will be to obtain fast slew rates in the presence of time delay and parametric uncertainty. At this design stage, there are no quantified control specifications defined. However, the general qualitative specifications apply to the design, i.e., fast slew rates, small steady state error and overshoot, and short settling time. The design will be approached using PI control based on tuning rules, Smith prediction, and robust control. Subsequently, the control law will be modified, perhaps by developing a switching controller, to ensure that stability and good performance are maintained even if hysteretic attachment occurs.

A. PI Control Using Tuning Rules

The PID controller and its variations (P, PI or PD) are the most commonly used controller in process control applications for the compensation of both delayed and non-delayed processes [7]. PID controllers display robustness to incorrect process model order assumptions and limited process parameter changes. Since derivative (D) control is sensitive to measurement noise, which is abundant in the CFTV system, PI controllers were designed based on a model of the CFTV system.

Because there are a large number of PI tuning rules available for first order plus time delay models, PI controllers were designed based on the first order model, $\frac{0.3618}{1.1194s+1}e^{-0.8806s}$, which resulted from using the two-point estimation method. This model was used because the corresponding simulated step responses match reasonably well with the test data as shown in Figure 9. Table III lists the parameters of the PI controller $K_c(1+\frac{1}{T_i s})$ for five different tuning rules. Figure 12 compares the closed-loop simulation results of the five PI tuning rules. It is clearly seen that the Abbas with 0% overshoot has the best performance. In Figure 12, the first order system obtained by two-point estimation was used in simulation.

TABLE III
PI CONTROLLER PARAMETERS USING DIFFERENT TUNING RULES

Tuning method	K_c	T_i
Ziegler-Nichols	3.1621	2.9324
Chien-Hrones-Reswick	1.2297	1.1194
Cohen and Coon	3.3915	1.1459
Haalman	2.3423	1.1194
Abbas (0% overshoot)	2.056	1.5597

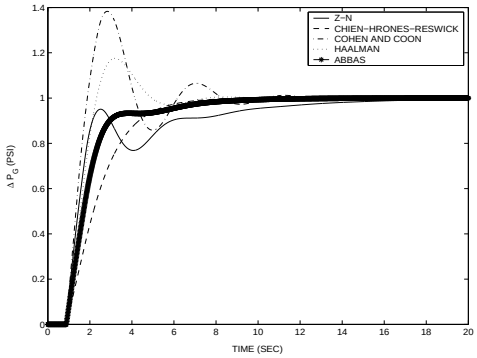

Fig. 12. PI controller performance comparison

PI controller can be considered as a baseline controller in the design. There is no doubt that the performance of this PI controller will be degraded in real system implementation. To compensate uncertainties in the real system, on-line adaptive tuning can be used.

B. Smith Predictor

Smith prediction is an effective methodology for compensating for system time delay. It has been seen that the performance of the Smith predictor for set point changes can be as much as 30% better than a conventional PID controller based on the ISE criterion [10]. It has also been seen that the Smith predictor can provide an improvement over PI control if the model parameters are within about 30% of the process parameters [10].

The adaptive Smith predictor [12] combines a standard Smith predictor along with an online process estimation method (e.g. the recursive least-squares method); hence the control parameters are updated as the process parameters are adaptively updated. Since the parameters of the CFTV system have been observed to change, an adaptive Smith predictor is expected to outperform either a standard PI controller or a fixed-gain Smith predictor.

C. Fixed-Architecture Robust Control

Fixed-architecture robust control, based on mixed structured singular value theory (MSSV) [13], [14] is an effective approach to developing practical control laws for systems with significant model uncertainty. This approach has the flexibility to develop control laws of a variety of structures, including PID and can be applied to CFTV control. The use of the MSSV yields much less conservative designs than those based on the small gain theorem, quadratic Lyapunov functions, or complex structured singular value theory.

D. Control in Presence of Hysteresis

Modeling of hysteresis for the CFTV system is a vital step in controller design. Many models have been proposed to describe hysteresis, including the Preisach model, the Krasnosel'skii-Pokrovskii operator, the Duhem hysteresis operator, and the Ishlinskii hysteresis operator [15], [16], [17]. Which model best matches the CFTV hysteresis remains to be determined. Modeling of CFTV hysteresis also includes studies of the dependency of hysteresis on the collar geometry and operating condition (e.g., the system set point).

The idea of inverse control for hysteresis is to construct an inverse operator to cancel out the hysteretic effect. But this compensation strategy is open-loop in nature and its effectiveness relies on the accuracy of the hysteresis modeling. Either adaptive control or robust control can be combined with inverse control to improve the performance of the compensation for the hysteresis [15], [17].

V. CONCLUSIONS

Recent engineering research has successfully demonstrated the potential of fluidic thrust vector control using counterflow at conditions up to Mach 2. However, feedback control has not been demonstrated using counterflow. The primary control objective is to achieve fast slew rates by compensating for the transportation delay, parameter uncertainties, and hysteresis. This paper has described an experimental testbed for investigating feedback control of CFTV. Initial system identification results were described along with preliminary PI control design, which will be used as a baseline controller. Potential control approaches for high performance control design were discussed.

REFERENCES

[1] P.J. Strykowski, A. Krothapalli, and D. J. Forliti, Counterflow Thrust Vectoring of Supersonic Jets, *AIAA Journal*, vol. 34, 1996, pp. 2306-2314.

[2] F.S. Alvi, P.J. Strykowski, A. Krothapalli, and D. J. Forliti, Vectoring Thrust in Multiaxes Using Confined Shear Layers, *ASME Journal of Fluids Engineering*, vol. 122, 2000, pp. 3-13.

[3] P.J. Strykowski and A. Krothapalli, "The Countercurrent Mixing Layer: Strategies for Shear-Layer Control," *in AIAA Shear Flow Conference*, Orlando, FL, 1993, AIAA 93-3260.

[4] J.D. Flamm, "Experimental Study of a Nozzle Using Fluidic Counterflow for Thrust Vectoring," *in the 34th AIAA/ASME/SAE/ASEE Joint Propulsion Conference & Exhibit*, Cleveland, OH, 1998, AIAA 98-3255.

[5] M.R. Van der Veer, *Counterflow Thrust Vectoring of a Subsonic Rectangular Jet*, M.S. Thesis, University of Minnesota, Minneapolis, MN; 1995.

[6] M. Maria, "Experimental Study on Counter-flow Thrust Vector Control of a Subsonic Rectangular Nozzle," *Technical Report*, Florida State University, 2000.

[7] K.J. Astrom and T. Hagglund, The Future of PID Control, *Control Engineering Practice*, vol. 9, 2001, pp. 1163-1175.

[8] Y. Nishikawa, N. Sannomiya, T. Ohta and H. Tanaka, A Method for Auto-tuning of PID Control Parameters, *Automatica*, vol. 20, no. 3, 1984, pp. 321-332.

[9] Q. Bi, W.J. Cai, E.L. Lee, Q.G. Wang, C. C. Hang and Y. Zhang, Robust Identification of First-order Plus Dead-time Model From Step Response, *Control Engineering Practice*, vol. 7, 1999, pp. 71-77.

[10] A. O'Dwyer, "A Survey of Techniques for the Estimation and Compensation of Process with Time Delay," *Technical Report AOD.00.03*, Dublin Institute of Technology, Ireland, 2000.

[11] C.T. Huang and C.J. Chou, Estimation of the Underdamped Second-order Parameters from the System Transient, *Industrial and Engineering Chemistry Research*, vol. 33, 1994, pp. 174-176.

[12] C.W. Alexander and R.E. Trahan Jr., A Comparison of Traditional and Adaptive Control Strategies for Systems with Time Delay, *ISA Transactions*, vol. 40, 2001, pp. 353-368.

[13] W.M. Haddad, D.S. Bernstein, and V. Chellabiona, Generalized Mixed-μ Bounds for Real and Complex Multiple-Block Uncertainty with Internal Matrix Structure, *International Journal of Control*, vol. 64, 1996, pp. 789-806.

[14] E.G. Collins, Jr., W.M. Haddad, L.T. Watson, and D. Sadhukhan, Probability-One Homotopy Algorithms for Robust Controller Synthesis with Fixed-Structure Multipliers, *International Journal of Robust and Nonlinear Control*, vol. 17, 1997, pp. 165-185.

[15] C.Y. Su, Y. Stepanenko, J. Svoboda and T. P. Leung, Robust Adaptive Control of a Class of Nonlinear Systems with Unknown Backlash-like Hysteresis, *IEEE Transactions on Automatic Control*, vol. 45, no. 12, 2000, pp. 2427-2432.

[16] J.W. Macki, P. Nistri and P. Zecca, Mathematical Models for Hysteresis, *SIAM Review*, vol. 35, no. 1, 1993, pp. 94-123.

[17] X. Tan, *Control of Smart Actuators*, Ph.D. Thesis, University of Maryland, College Park, MD; 2002.